

Contents

Contents	I
1 Physical Background	1
1.1 Born-Oppenheimer Approximation	1
1.2 Molecular Term Symbol	1
1.3 Electronic transitions	1
1.4 Franck-Condon Principle	2
1.5 Morse-Potential	3
1.6 Birge-Sponer Method	4
2 Setup and Implementation	5
2.1 Setup	5
2.2 Implementation	6
3 Analysis	7
3.1 Analysis of the Absorption-Spectrum	7
3.1.1 Calculation of the Potential Depth	9
3.1.2 Calculation of the Dissociation Energy	10
3.1.3 Calculation of the Excitation Energy	11
3.1.4 The Morse-Potential	11
3.2 Analysis of the Emission Spectrum	12
3.2.1 The Emission Spectrum	14
4 Discussion	15
4.1 Absorption Spectrum	15
4.2 Emission Spectrum	16
A Appendix	17
List of Figures	17
List of Tables	17
References	18

1 Physical Background

1.1 Born-Oppenheimer Approximation

The Born-Oppenheimer approximation assumes that the motion of nuclei and electrons in a molecule can be described separately. As electrons are much lighter and move faster than nuclei, their equations of motion can be solved with no remark to the nuclei. Therefore, the wave function ψ_{mol} can be approximated by a product of two independent wave functions:

$$\psi_{\text{mol}}(r_i, R_j) = \psi_{\text{vib}}(R_j) \cdot \psi_{\text{el}}(r_i, R_j), \quad (1)$$

where ψ_{vib} describes the nuclei and ψ_{el} the electrons.

1.2 Molecular Term Symbol

To characterize a state of a molecule and give a short overview of the quantum numbers, the so called molecular term symbol can be used:

$${}^{2S+1}\Lambda_{\Omega, (g/u)}^{(+/-)}. \quad (2)$$

In this notation,

- S is the total spin quantum number and the whole term $2S+1$ gives the multiplicity,
- Λ refers to the projection of the orbital angular momentum along the internuclear axis and for $\Lambda = 0, 1, 2, \dots$ we write $\Sigma, \Pi, \Delta,$
- Ω gives the total angular momentum projected on the internuclear axis,
- g/u for *gerade* and *ungerade* (even and odd) represent the effect of the point mirroring operation \hat{i} ,
- $+/-$ are used to describe the effect of mirroring along a plane around the internuclear axis.

As the electronic states are not part of the notation, they are often added by a capital letter directly in front of the term symbol. The electronic ground state is labelled X and the excited states are labelled with A, B, C, \dots in their energetic order.

1.3 Electronic transitions

The ground state of the iodine molecule is ${}^1\Sigma_{0,g}^+$. To find possible transitions, the selection rules for electronic transitions

- $g \leftrightarrow u, g \leftrightarrow g, u \leftrightarrow u$
- $\Delta\Omega = 0, \pm 1$
- $\Delta\Lambda = 0, \pm 1$

are applied. The third rule can be applied because of the strong spin-orbit interaction. Using these rules in respect of the transitions that can be observed with the used spectrometer only one transition will be measured:

$$X^1\Sigma_{0,g}^+ \leftrightarrow B^3\Pi_{0,u}^+. \quad (3)$$

The observed electronic transition consists out of a system of vibrational transitions. For a spectrometer with a better resolution the rotational transitions, would be interesting as for every vibrational transition several rotational lines could be observed. With the setup used in the experiment, this resolution is not possible, so the rotational transitions are not relevant.

1.4 Franck-Condon Principle

The Franck-Condon principle is used to explain the intensity of different vibronic transitions. As vibronic transitions are very fast compared to the movement of the nuclei, transitions where the nuclear position changes the least appear more likely (cf. fig. 1). Therefore if the vibrational wave functions overlap more the intensity of the corresponding transition will be higher. The overlap of the two vibrational wave functions can be calculated and is called the Frank-Condon factor:

$$FC(\nu, \nu') = \left| \int \psi_\nu \psi_{\nu'} dr \right|^2. \quad (4)$$

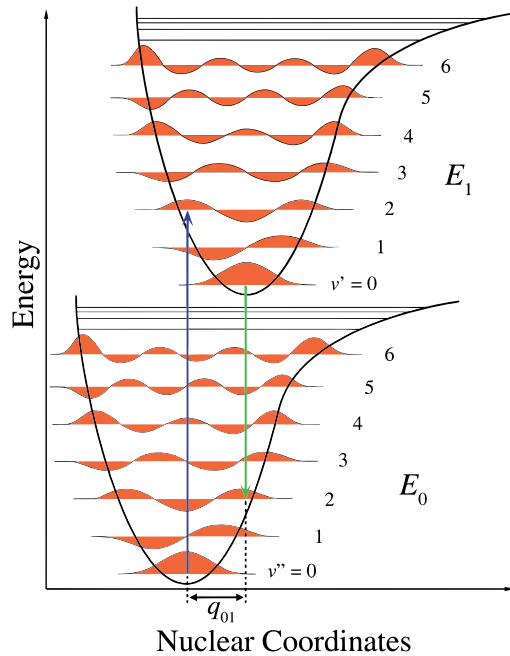


Figure 1: In the diagram, an electronic transition from the ground state to the first excited state is shown. Two different transitions in the vibronic state are shown and one can see that the transitions occur straight without a change in the nuclear coordinates.

1.5 Morse-Potential

The Morse-potential

$$V(r) = D_e(1 - \exp(-a(r - r_e)))^2$$

with $r_e = 2.979 \text{ \AA}$

(5)

approximates the potential energy of a molecule. It approximates the vibrational structure of a molecule much better than approximating the potential energy with the quantum harmonic oscillator (see fig. 2) as it also includes more effects. Approximating with the Morse potential also takes possible bond breaking and unbound states into account.

Solving the Schrödinger equation with the Morse potential yields

$$\frac{E_{\text{vib}}}{hc} = \omega_e \left(n + \frac{1}{2} \right) - \omega_e x_e \left(n + \frac{1}{2} \right)^2.$$
(6)

The molecular constants are given by

$$\omega_e = a \sqrt{\frac{\hbar D_e}{\pi c \mu}},$$

$$\omega_e x_e = \frac{\hbar a^2}{4\pi c \mu},$$
(7)

where μ is the reduced mass and a a constant. By eliminating the constant a the dissociation energy can be calculated with

$$D_e = \frac{\omega_e^2}{4\omega_e x_e}.$$
(8)

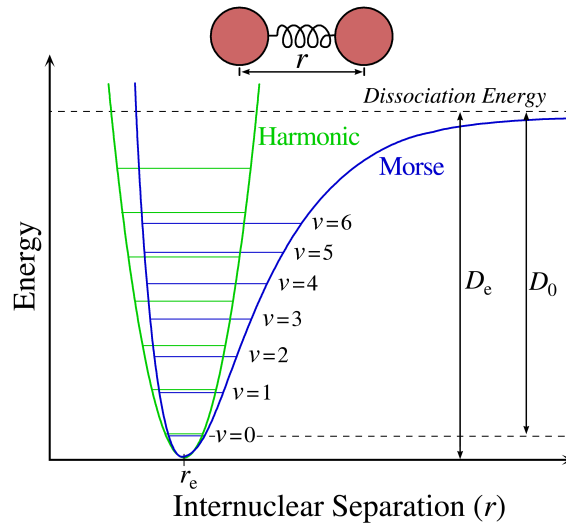


Figure 2: In the graphic, the difference between the quantum harmonic oscillator approximation of the potential and the Morse potential is shown. One can see the difference in the vibrational levels for the different approximations.

1.6 Birge-Sponer Method

The energy for vibration and rotation in molecules is quantized. Approximating the potential to determine the allowed energies to the vibronic states yields:

$$G(\nu) = \omega_e \left(\nu + \frac{1}{2} \right) - \omega_e x_e \left(\nu + \frac{1}{2} \right)^2. \quad (9)$$

The parameters ω_e and $\omega_e x_e$ are molecule constants that can be determined with use of the Birge-Sponer method. The Birge-Sponer method determines the molecule constants and the dissociation energy by calculating the difference between the levels with

$$\Delta G_{\nu+\frac{1}{2}} = G \left(\nu + \frac{1}{2} \right) - G(\nu) = \omega_e - \omega_e x_e (2\nu + 2). \quad (10)$$

With the maximum of the sum at ν_{\max} , the dissociation energy of the ground state can be found with

$$D_0 = \sum_{\nu=0}^{\nu_{\max}} \Delta G_{\nu+\frac{1}{2}}. \quad (11)$$

To calculate the dissociation energy relative to the minimum of the potential, the zero-point energy has to be added:

$$D_e = D_0 + G(0). \quad (12)$$

To provide some further visualisation of the discussed quantities one can take a look at fig. 3.

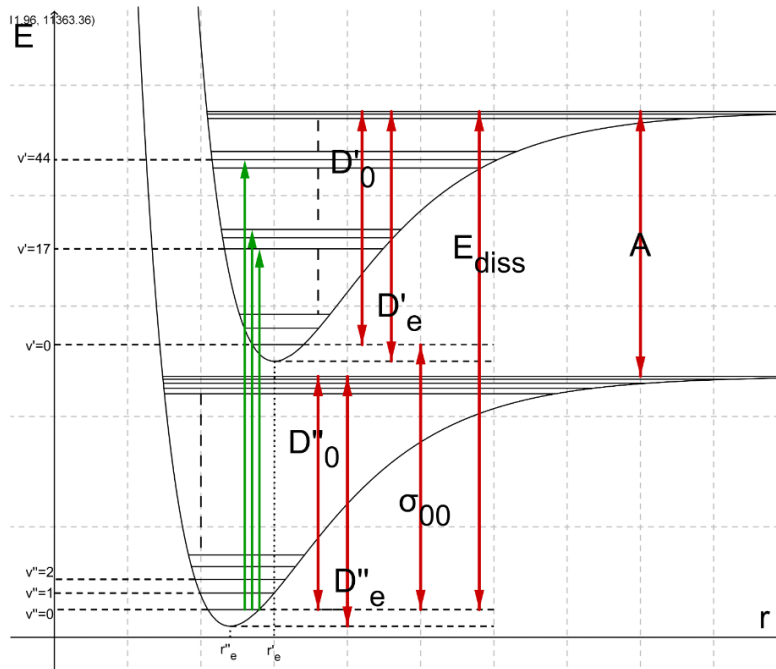


Figure 3: In this figure the discussed quantities are visualised.

2 Setup and Implementation

2.1 Setup

The setup that is shown in fig. 4 contains everything needed for both parts of the experiment.

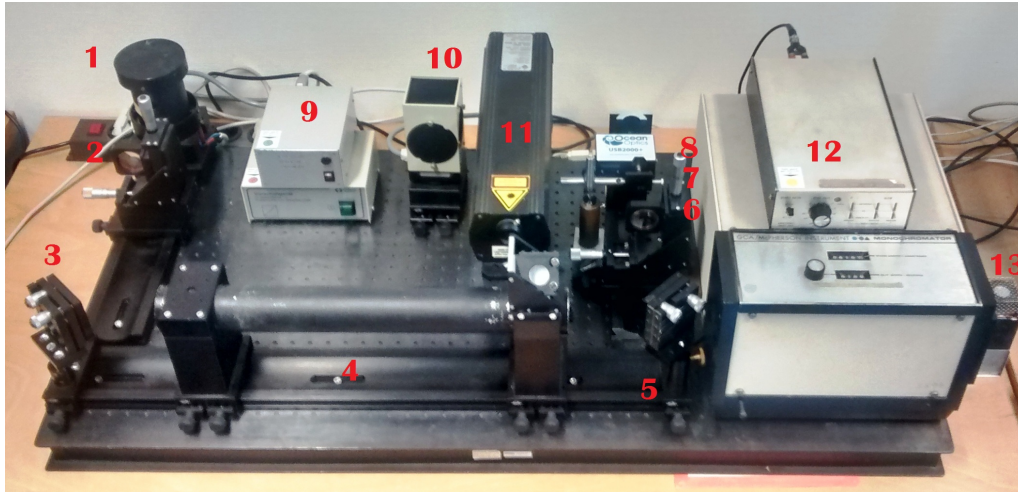


Figure 4: Setup of the experiment, 1: halogen lamp, 2: lens, 3:mirror, 4:iodine-tube, 5: mirror, 6: lens, 7: filter, 9: power supply for the lamps, 10: mercury lamp, 11: helium-neon laser, 12: monochromator, 13: photomultiplier. In the actual setup the filter does not exist anymore

Measuring the Absorption Spectra For the first part of the experiment the setup is used as shown in fig. 4. The halogen lamp is adjusted in a way that the light is focussed by the first lens (150 mm) and reflected into the iodine-tube with help of the mirror. The light that comes out of the iodine-tube is reflected by a second mirror and focused on the CCD-spectrometer with help of a second lens (70 mm).

Calibration of the Monochromator For calibrating the monochromator the halogen lamp is replaced with the mercury lamp. Furthermore the second mirror is taken out of a setup and its place is taken by the second lens so the light that passes the iodine-tube is focused on the monochromator. The signal of the monochromator is amplified by a photomultiplier.

Measuring the Emission Spectra To measure the emission spectra, the mercury lamp is switched off and the laser is focused on the iodine-tube. Same as for calibrating, the light that comes out of the iodine-tube is focused on the monochromator.

The signal from the monochromator as well as the signal of the CCD-spectrometer can be read out on the computer. Next to the experimental setup, the Peltier-cooling for the photomultiplier, its power-supply and the discriminator are placed.

2.2 Implementation

Measuring the Absorption Spectra Using the setup as described before, first of all the optical path is checked and optimized by moving the lenses and mirrors a little. Then the program SpectraSuite was opened and the small blind in front of the laser was adjusted until a nice spectrum was visible. For the measurement, the integration time was chosen as 100 ms and 10 000 scans for average was chosen to smooth the curve.

Calibrating the Monochromator To calibrate the monochromator, the setup was changed as described above and the optical path was checked and optimized again. The program Jod-analog.vi was started and the spectrum for wavelengths 4000 Å to 6000 Å was measured. Measuring a spectrum means that on the monochromator a starting point and a step width was chosen. For the calibration, the starting point was 4000 Å and the step width 2 Å. This starting point was also set in the program in a small window that appears after switching the parameter-lever. On the discriminator, different settings could be changed. Firstly, the range was adjusted so the signal does not over modulate and the discriminator level was used to do fine adjustments. For the calibration, the discriminator was set to 0.4 and the range was chosen to 1 000 000. Then the program and the monochromator were started and stopped when the monochromator has reached 6000 Å. The exact wavelengths for start and stop that were shown on the monochromator were noted as the values shown by the program are not accurate.

Measuring the Emission Spectra The setup was changed to the third one and again the optical path was checked.

Firstly, the laser-peak was measured with a step width of 2 Å, start- and stop-wavelength at 6300 Å and 6400 Å, range of 3 000 000 and discriminator level of 0.4. The slit width of the monochromator was set to 50 µm. The measured data were saved and the relevant wavelengths noted.

Secondly the fluorescent-spectra was measured. To do so, the step width was set to 1 Å, start- and stop-wavelengths to 6400 Å and 8000 Å, respectively, and a range of 1000 and discriminator level of 0.4. The slit-width was changed to 370 µm.

For all measurements, a hairdryer was used to heat to iodine-tube. For measuring the emission-spectra, the room was shaded.

3 Analysis

3.1 Analysis of the Absorption-Spectrum

To analyze the vibration behavior of the iodine molecule, the absorption-spectrum was measured. To identify a certain transition, a wavelength of $\lambda_{25} = 545.8$ nm for the $\nu'' = 0 \rightarrow \nu' = 25$ transition was given. The measured spectrum is shown in fig. 5. To determine

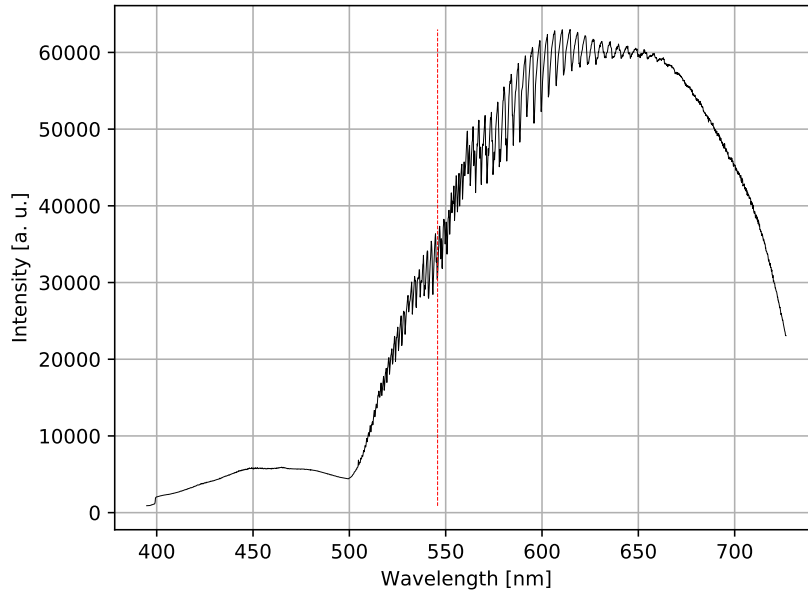


Figure 5: In this graph, the measured spectrum is displayed. The given reference wavelength is marked with a vertical red line.

the values for $\omega_e x_e$ and ω_e , the linearity of the dependency between ΔG and $\nu + 1/2$ is used. The given transition is used to identify other transitions of the $\nu'' = 0$ progression. The corresponding wavelengths are used to calculate the differences between the transitions and plot them against the vibration quantum number ν' in the so called Birge-Sponer-Plot. The used wavelengths are marked in fig. 6. To calculate ΔG ,

$$\Delta G = \frac{1}{\lambda_{\nu'+1}} - \frac{1}{\lambda_{\nu'}} \quad (13)$$

was used. The error on ΔG is given by Gaussian error propagation using the estimated error $s_\lambda = 0.1$ nm.

$$s_{\Delta G} = \sqrt{\left(\frac{s_\lambda}{\lambda_{\nu'+1}^2}\right)^2 - \left(\frac{s_\lambda}{\lambda_{\nu'}^2}\right)^2} \quad (14)$$

The Birge-Sponer-Plot is shown in fig. 7. To determine $\omega_e x_e$ and ω_e , a linear regression of the form

$$f(x) = mx + c \quad (15)$$

is made. The fit parameters were calculated by using the function `curve_fit` from the python module `scipy.optimize` which uses the method of least squares. The fitted pa-

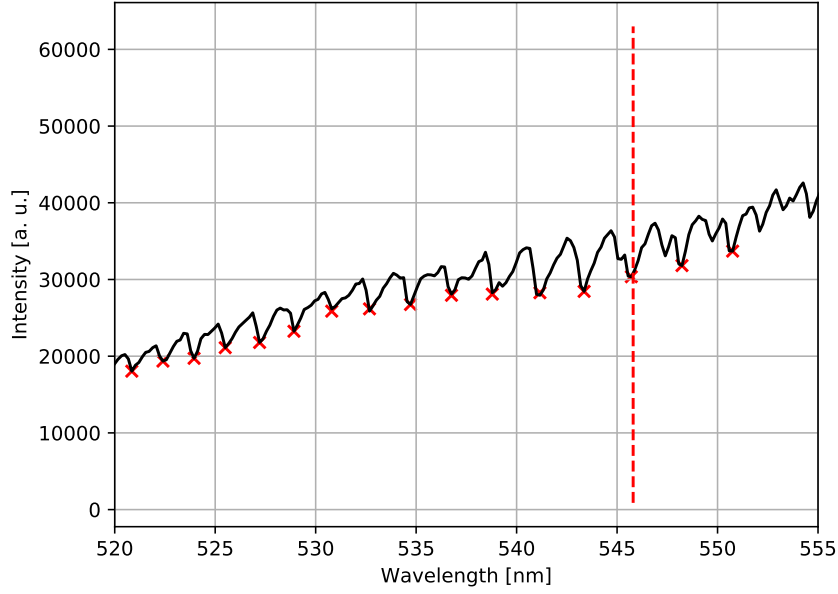


Figure 6: In this figure the used wavelengths are marked with crosses and the reference-wavelength is marked with a line.

rameters are:

$$m = (-2.11 \pm 0.15) \frac{1}{\text{cm}} \quad c = (133 \pm 5) \frac{1}{\text{cm}}. \quad (16)$$

If one compares the linear fit to eq. (10), it can be seen that $\omega_e x_e$ can be calculated by

$$\omega_e x_e = -\frac{m}{2}. \quad (17)$$

With Gaussian error propagation one finds that the error is given by

$$s_{\omega_e x_e} = \frac{s_m}{2}. \quad (18)$$

So for the value of $\omega_e x_e$,

$$\omega_e x_e = (1.05 \pm 0.08) \frac{1}{\text{cm}} \quad (19)$$

was calculated. For the calculation of ω_e ,

$$\Delta G\left(\nu + \frac{1}{2}\right) = \underbrace{\omega_e - \omega_e x_e}_c - \underbrace{2\omega_e x_e}_m \left(\nu + \frac{1}{2}\right) \quad (20)$$

is used so it is easily seen that ω_e is given by

$$\omega_e = c + \omega_e x_e \quad (21)$$

with an error calculated by

$$s_{\omega_e} = \sqrt{s_c^2 + s_{\omega_e x_e}^2}. \quad (22)$$

Finally for the value, we obtain

$$\omega_e = (135 \pm 5) \frac{1}{\text{cm}}. \quad (23)$$

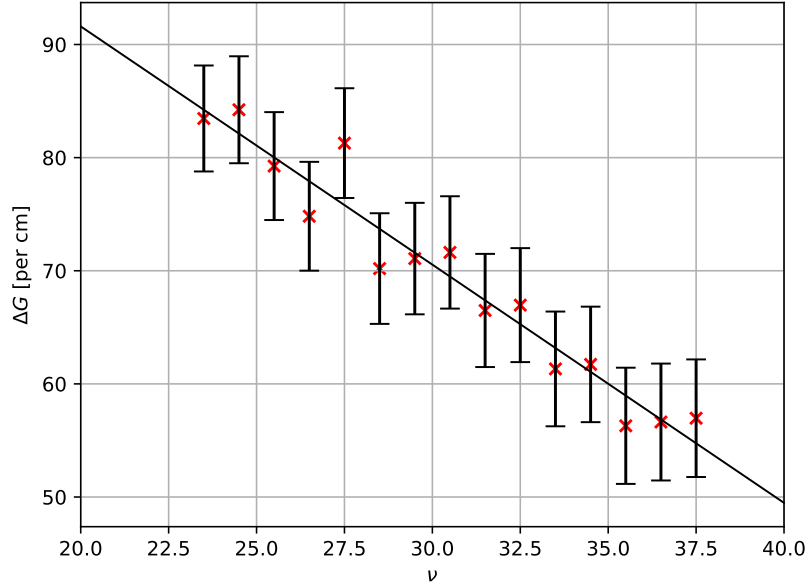


Figure 7: In this picture the linear regression and the Birge-Sponer-Plot are displayed

3.1.1 Calculation of the Potential Depth

The potential depth is going to be calculated in two different ways. Firstly, using the Morse-Potential approximation which delivers

$$D'_e = \frac{\omega_e^2}{4\omega_e x_e}. \quad (24)$$

Using Gaussian error propagation for the uncertainty,

$$s_{D'_e} = \sqrt{\left(\frac{\omega_e}{2\omega_e x_e} s_{\omega_e}\right)^2 + \left(\frac{\omega_e^2}{4(\omega_e x_e)^2} s_{\omega_e x_e}\right)^2}. \quad (25)$$

was used. So for the value of the potential depth,

$$D'_{e,1} = (4313 \pm 428) \frac{1}{\text{cm}}. \quad (26)$$

is determined. The second option to calculate the potential depth is to use the term differences. We know that the potential depth is the sum of all term differences of a shared electronic state. This sum can be approximated by the area under the straight line of the Birge-Sponer-Plot as shown in the equation below:

$$D'_e = \sum_{\nu'=0}^{\nu'_{\text{diss.}}} \Delta G'(\nu' + \frac{1}{2}) + G(0) \approx \frac{c\nu'_{\text{diss.}}}{2}. \quad (27)$$

To determine the potential depth, the critical value for ν' called $\nu'_{\text{diss.}}$ which is given as the zero point of the linear function yielded by the linear regression is needed. So

$$0 = m \left(\nu'_{\text{diss.}} + \frac{1}{2} \right) + c \quad (28)$$

$$\implies \nu'_{\text{diss.}} = -\frac{c}{m} - \frac{1}{2} \quad (29)$$

with an error determined by Gaussian error propagation of

$$s_{\nu'_{\text{diss.}}} = \sqrt{\left(\frac{1}{m} s_c\right)^2 + \left(\frac{c}{m^2} s_m\right)^2} \quad (30)$$

is used. Finally, the value of $\nu'_{\text{diss.}}$ is calculated to be

$$\nu'_{\text{diss.}} = 63 \pm 5 \quad (31)$$

which leads to a value for the potential depth of

$$D'_{e,2} = (4212 \pm 368) \frac{1}{\text{cm}}. \quad (32)$$

The error was calculated by Gaussian error propagation which delivered the following equation:

$$s_{D'_{e,2}} = \frac{1}{2} \sqrt{(c \cdot s_{\nu'_{\text{diss.}}})^2 + (\nu'_{\text{diss.}} \cdot s_c)^2} \quad (33)$$

3.1.2 Calculation of the Dissociation Energy

The dissociation energy is the energy needed for a photon to cause the molecule to dissociate. Since the electric state must change if the molecule gets excited by a photon, the dissociation energy is not just the depth of the potential. The dissociation energy can easily be determined by looking at the absorption spectrum and searching for the lowest wavelength where no absorption peak is observed. The chosen wavelength is, as shown in fig. 8, $\lambda = (500 \pm 2)$ nm. Therefore, the dissociation energy can be calculated by

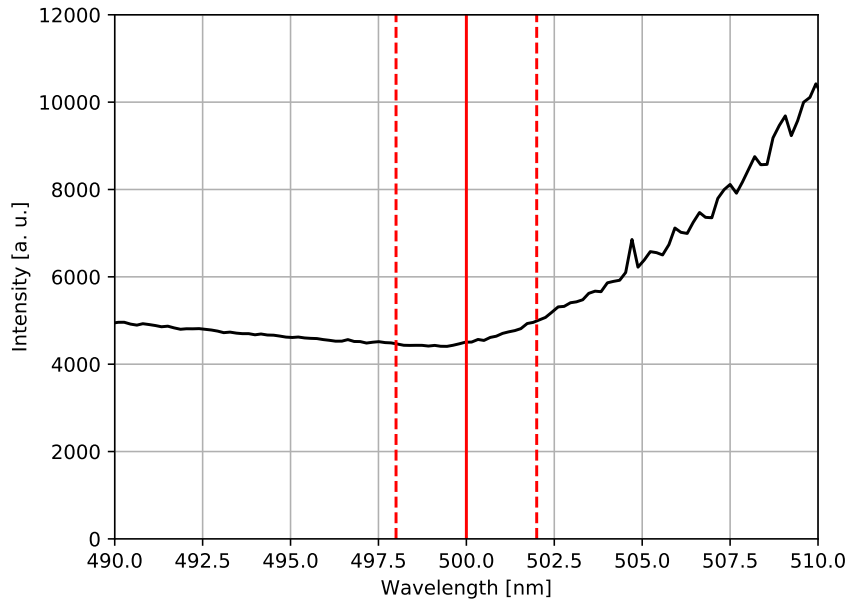


Figure 8: In this picture the estimation of the dissociation energy is displayed

$E_{\text{diss.}} = 1/\lambda$ with an error of $s_{E_{\text{diss.}}} = s_{\lambda}/\lambda^2$. The value was determined to be

$$E_{\text{diss.}} = (20\,000 \pm 80) \frac{1}{\text{cm}}. \quad (34)$$

3.1.3 Calculation of the Excitation Energy

The excitation energy T_e is the energy gap between $\nu' = 0$ and $\nu'' = 0$. The equation used to calculate the excitation energy is

$$E_{\text{diss.}} = T_e - G''(0) + D'_e \quad (35)$$

$$\approx T_e - G'(0) + D'_e \quad (36)$$

$$= T_e + D'_0. \quad (37)$$

Since $G''(0)$ is unknown, it has to be approximated by $G'(0)$. To do further calculations, the value for D'_0 is needed. It is calculated by

$$D'_0 = D'_e - G'(0) = (4129 \pm 48) \frac{1}{\text{cm}}, \quad (38)$$

where instead of D'_0 , the already calculated $D'_{e,1}$ is used. Using these values,

$$T_e = E_{\text{diss.}} - D'_0 = (15\,553 \pm 435) \frac{1}{\text{cm}} \quad (39)$$

was determined for the excitation energy where the error is calculated by Gaussian error propagation with

$$s_{T_e} = \sqrt{s_{E_{\text{diss.}}}^2 + s_{D'_0}^2}. \quad (40)$$

3.1.4 The Morse-Potential

Using the values determined earlier for $\omega_e x_e$ and $D'_{e,1}$, it is now possible to plot the so determined Morse-Potential of the form

$$V(R) = D'_{e,1} \cdot (1 - \exp(-a(R - R_e)))^2. \quad (41)$$

a is calculated by

$$a = \sqrt{\frac{4\pi c \mu \cdot \omega_e x_e}{\hbar}} \quad (42)$$

where \hbar is the reduced Planck constant, μ is the reduced mass of the iodine molecule and c is the speed of light. It is important to be aware of the units during this calculation. The computed plot is displayed in fig. 9.

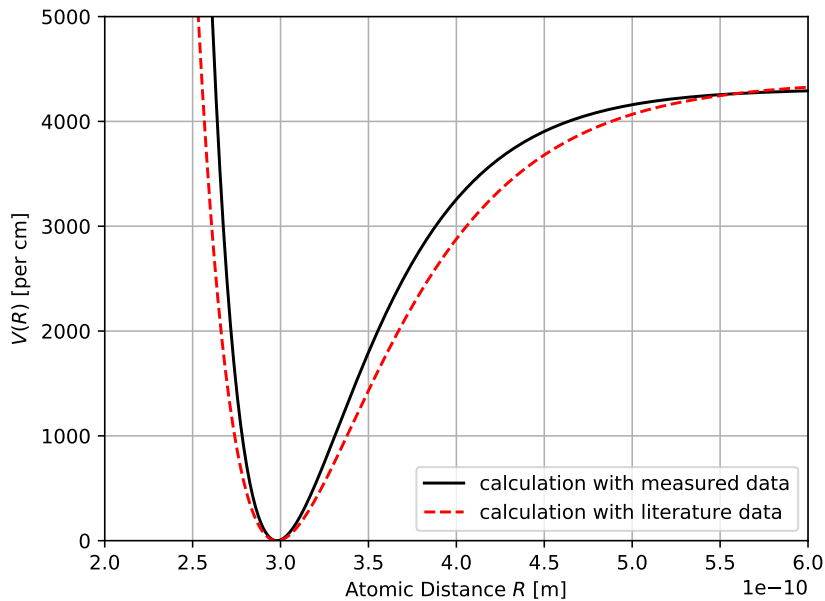


Figure 9: In this figure the determined Morse-Potential is displayed. For comparison also the Morse-Potential using the literature values was computed.

3.2 Analysis of the Emission Spectrum

In this part of the experiment, a monochromator was used. Since the measuring program is not able to measure the wavelength properly, a correction is needed. Therefore, the starting point and the ending point of a measurement was noted and the measured intensities are plotted against a linear scaled set of generated data between the starting and the ending point of the measurement.

For the measurement of the emission spectrum, a calibration measurement was executed. This calibration uses a Hg-lamp which emits a discrete and very well known spectrum so one can compare the measured spectrum with the expected one and is therefore able to correct possible scalings and off-sets. As shown in fig. 10, the measured spectrum fits the expected one quite well, but since the resolution of measured spectrum is not high enough it was not possible to see any needed correction.

The used He-Ne-laser is expected to emit light with a wavelength of $\lambda = 6330 \text{ \AA}$. The spectrum of the laser to determine the molecular transition of iodine when irradiated by the laser light was measured. As shown in fig. 11 the spectrum of the laser was neither as sharp nor as Gaussian shaped as expected so it was not possible to determine a certain wavelength.

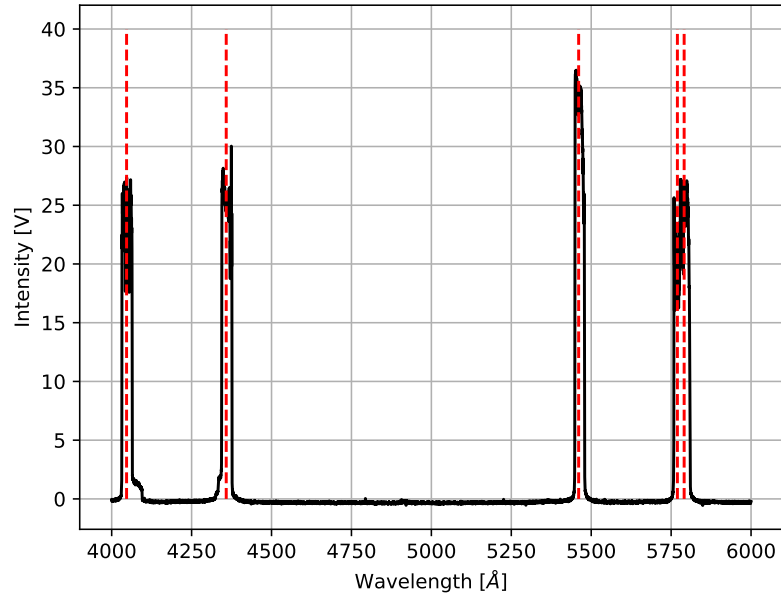


Figure 10: In this picture the measured spectrum is displayed. For comparison the expected emission lines of the Hg-lamp are displayed too.

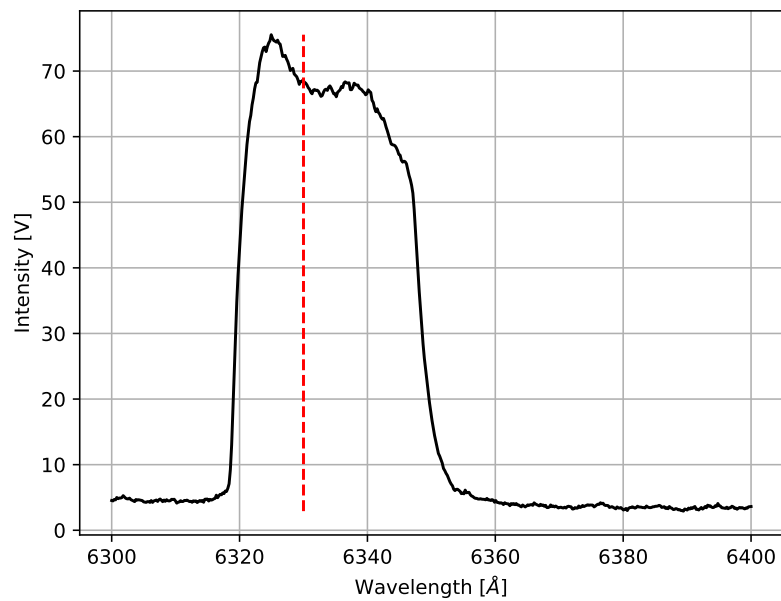


Figure 11: In this figure the measured spectrum emitted by the laser is displayed. For comparison, the expected wavelength is shown.

3.2.1 The Emission Spectrum

The measurement of the emission spectrum does not show enough precision to find a sensitive fit function for the peaks. Therefore, to determine the peaks and the corresponding wavelengths, the maxima were approximated. The data and the determined peaks are displayed in fig. 12. Below the determined peak positions are listed. The errors where

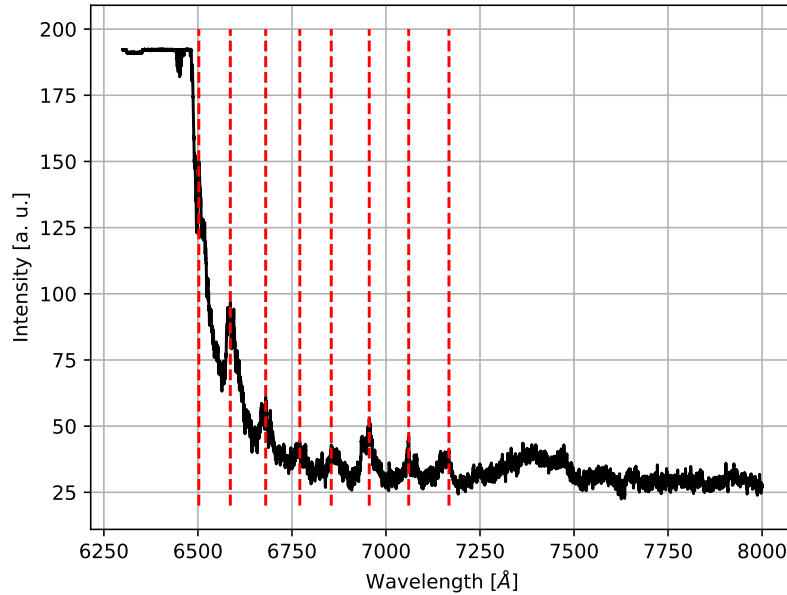


Figure 12: In this figure the measured emission spectrum is displayed. In red the estimated peak locations are marked.

determined by estimating the half peak width as this seemed to give sensitive values in respect to the noisy data.

$$\begin{aligned}
 \lambda_1 &= (6502 \pm 4) \text{ \AA} & \lambda_5 &= (6855 \pm 15) \text{ \AA} \\
 \lambda_2 &= (6590 \pm 10) \text{ \AA} & \lambda_6 &= (6960 \pm 20) \text{ \AA} \\
 \lambda_3 &= (6680 \pm 10) \text{ \AA} & \lambda_7 &= (7060 \pm 20) \text{ \AA} \\
 \lambda_4 &= (6771 \pm 15) \text{ \AA} & \lambda_8 &= (7167 \pm 20) \text{ \AA}
 \end{aligned}$$

To determine the measured progression by comparing the wavelengths to literature values, it helps to calculate the wave numbers $k = 1/\lambda$. The error is given by Gaussian error propagation $s_k = s_\lambda/\lambda^2$. The so computed values are listed in table 1. By comparing the measured wave numbers and the values in [FP] it was seen that the measured emission-peaks are most probably caused by the $\nu' = 6 \rightarrow \nu'' = 5 \dots 12$ progression.

ν''	$k_{\text{meas.}} [\frac{1}{\text{cm}}]$	$k_{\text{lit.}} [\frac{1}{\text{cm}}]$
5	$15\,379 \pm 9$	15 394
6	$15\,183 \pm 23$	15 187
7	$14\,970 \pm 22$	14 981
8	$14\,770 \pm 30$	14 776
9	$14\,590 \pm 30$	14 572
10	$14\,380 \pm 40$	14 370
11	$14\,160 \pm 40$	14 169
12	$13\,950 \pm 40$	13 969

Table 1: In this table the measured wave numbers are listed

4 Discussion

4.1 Absorption Spectrum

In the first part of the experiment, the absorption spectrum of the iodine molecule was measured. To do so, a halogen lamp and a CCD-spectrometer were used. The measured spectrum shows the expected absorption minimums and the given transition could be identified and used to determine further dips resulting from the zeroth progression between the $X^1\Sigma_{0g}^+$ and the $B^3\Pi_{0u}^+$ state of the iodine molecule. The Birge-Sponer method has been used to determine two molecular constants:

$$\omega_e x_e = (1.05 \pm 0.08) \frac{1}{\text{cm}} \quad (43)$$

and

$$\omega_e = (135 \pm 5) \frac{1}{\text{cm}}. \quad (44)$$

The literature values [SC] for these two constants are

$$\omega_e x_e = (0.7016 \pm 0.0100) \frac{1}{\text{cm}} \quad (45)$$

and

$$\omega_e = (125.273 \pm 0.100) \frac{1}{\text{cm}}. \quad (46)$$

Even though the spectrum looked really promising, the determined values for the molecular constants are not that satisfying. The relative uncertainties of the values in respect to the rough measuring setup are in a sensitive range. Nevertheless, the determined values do not fit the literature values. One reason for this could be that the location of the dips is not easy to determine. Even though the dips were not determined by eye but analytically, a small change in the location of a dip changes the output of the Birge-Sponer plot significantly. As this error can not really be quantized it was neglected in the further analysis. So finding a better method to determine the location of the dips or at least a way to include the error would most probably yield better results.

Furthermore, the potential depth of the excited state was calculated twice using two different methods. Firstly, it was calculated by using the Morse potential approximation that lead to

$$D'_{e,1} = (4313 \pm 428) \frac{1}{\text{cm}}. \quad (47)$$

Secondly, the value was calculated by determining the area enclosed by the line in the Birge-Sponer plot. The second method yields

$$D'_{e,2} = (4212 \pm 368) \frac{1}{\text{cm}}. \quad (48)$$

The literature value for the potential depth [SC] is $D'_{e,\text{lit}} = 4391 \frac{1}{\text{cm}}$. Comparing the values, the experimentally determined values are in a very nice magnitude and both hit the literature value within one standard derivation. Surprisingly, the second method does not give a better value than approximating with help of the Morse-potential. A reason for this could be that the fitted line underestimates the real area.

The excitation energy was determined to

$$E_{\text{diss.}} = (20\,000 \pm 80) \frac{1}{\text{cm}} \quad (49)$$

while the literature [SC] gives $E_{\text{diss., lit}} = 20\,014 \frac{1}{\text{cm}}$ for the excitation energy. Therefore, the determined value is in a 1σ -neighborhood. Also, the relative error is of satisfying order.

Lastly, the dissociation energy was used to determine the energy T_e which is the energy difference between the potential minima of the two states. The calculated value is

$$T_e = E_{\text{diss.}} - D'_0 = (15\,553 \pm 435) \frac{1}{\text{cm}} \quad (50)$$

and the literature [SC] gives $T_{e,\text{lit}} = 15\,770.59 \frac{1}{\text{cm}}$. Again, the calculated value is in a good 1σ -range in respect to the literature value.

With use of the calculated values, the Morse potential was calculated and plotted in comparison to the Morse potential plotted with use of the literature values. As seen in fig. 2, the calculated Morse potential shows a very satisfying result. For the asymptotic part of the potential curve the measured and literature curve differ a little but with the calculated values it should be in one standard deviation.

4.2 Emission Spectrum

In the second part of the experiment, the emission of the iodine molecule was measured by exciting it with a laser and measuring the spectrum with a monochromator. The location of the peaks were determined and the measured values were compared to wave numbers one would expect for different progressions. By comparison, it was found that most likely the $\nu' = 6 \rightarrow \nu'' = 5 \dots 12$ progression has been measured. The measured data and the expected data for that progression are listed in table 2. The measured values are all in a 1σ -range of the expected ones with respect to the chosen progression. Also, the error is in a sensitive range. Nevertheless, it would be really nice and most probably yield better results to be able to use a better spectrometer as the work with the monochromator is not really pleasing and the data is interstratified by a lot of random noise.

ν''	$k_{\text{meas.}} [\frac{1}{\text{cm}}]$	$k_{\text{lit.}} [\frac{1}{\text{cm}}]$
5	$15\,379 \pm 9$	15 394
6	$15\,183 \pm 23$	15 187
7	$14\,970 \pm 22$	14 981
8	$14\,770 \pm 30$	14 776
9	$14\,590 \pm 30$	14 572
10	$14\,380 \pm 40$	14 370
11	$14\,160 \pm 40$	14 169
12	$13\,950 \pm 40$	13 969

Table 2: The measured wave numbers in comparison to the expected ones if the right transition was chosen.

A Appendix

List of Figures

1	Frank-Condon-Principle	2
2	Morse-Potential	3
3	In this figure the discussed quantities are visualised.	4
4	Setup of the experiment, 1: halogen lamp, 2: lens, 3:mirror, 4:iodine-tube, 5: mirror, 6: lens, 7: filter, 9: power supply for the lamps, 10: mercury lamp, 11: helium-neon laser, 12: monochromator, 13: photomultiplier. In the actual setup the filter does not exist anymore	5
5	In this graph, the measured spectrum is displayed. The given reference wavelength is marked with a vertical red line.	7
6	In this figure the used wavelengths are marked with crosses and the reference-wavelength is marked with a line.	8
7	In this picture the linear regression and the Birge-Sponer-Plot are displayed	9
8	In this picture the estimation of the dissociation energy is displayed	10
9	In this figure the determined Morse-Potential is displayed. For comparison also the Morse-Potential using the literature values was computed.	12
10	In this picture the measured spectrum is displayed. For comparison the expected emission lines of the Hg-lamp are displayed too.	13
11	In this figure the measured spectrum emitted by the laser is displayed. For comparison, the expected wavelength is shown.	13
12	In this figure the measured emission spectrum is displayed. In red the estimated peak locations are marked.	14

List of Tables

1	In this table the measured wave numbers are listed	15
2	The measured wave numbers in comparison to the expected ones if the right transition was chosen.	17

References

- [FP] *"Fortgeschrittenen Praktikum Teil 1, Spektroskopie am Jod-Molekül, M.Meyer"*
10/2014
- [FC] *"Samoza, CC BY-SA 3.0, <https://commons.wikimedia.org/w/index.php?curid=33461268>",*
10/03/2019
- [MP] [https://en.wikipedia.org/wiki/Morse_potential#/media/File:](https://en.wikipedia.org/wiki/Morse_potential#/media/File:Morse-potential.png)
Morse-potential.png, 10/04/2019
- [SC] *"Spectroscopic Constants and Vibrational Assignment for the $B^3\Pi_{0u}^+$ State of Iodine,*
J. I. Steinfeld, R. N. Zare, L. Jones, M. Lesk and W. Klemperer, The Journal of
Chemical Physics 42, 25", 1965

Iodine

Kali 1	4000 Å	-	6000 Å	(Hull)	10 Å/s
Kali 2	4000	-	6000 Å	(gut)	2 Å/s
Kiesel	6300	-	6400		2 Å/s
Jed	6300	-	8000	1000 range	1 Å/s
Jed 2	6300	-	8000	300 range	1 Å/s

Freitag Absorption

of 500 samples

1000000 μs Int 20.1

Amos M. K. K. K.
04.10.2019